


# Network pharmacology-based dissection of the underlying mechanisms of dyspnoea induced by zedoary turmeric oil

Zhirui Yang<sup>1,2</sup> | Zhenzhen Wang<sup>1,2</sup> | Jiangling Li<sup>3</sup> | Jianglan Long<sup>1,2</sup> | Cheng Peng<sup>3</sup> | Dan Yan<sup>1,2</sup> 

<sup>1</sup>Beijing Institute of Clinical Pharmacy, Beijing Friendship Hospital, Capital Medical University, Beijing, China

<sup>2</sup>Beijing Key Laboratory for Evaluation of Rational Drug Use, Beijing Shijitan Hospital, Capital Medical University, Beijing, China

<sup>3</sup>School of Pharmacy, Chengdu University of Traditional Chinese Medicine, Chengdu, China

## Correspondence

Cheng Peng, School of Pharmacy, Chengdu University of Traditional Chinese Medicine, Chengdu 611137, China.

Email: pengc028@126.com

Dan Yan, Beijing Institute of Clinical Pharmacy, Beijing Friendship Hospital, Capital Medical University, Beijing 100050, China.

Email: pharmsci@126.com

## Funding information

Beijing Excellent Talent Project, Grant/Award Numbers: 2018000021223TD09, DFL20190702; National Key R&D Program of China, Grant/Award Number: 2020YFF01014606; National Natural Science Foundation of China, Grant/Award Numbers: 81773891, 82130112

## Abstract

Zedoary turmeric oil (ZTO) has been widely used in clinic. However, the unpleasant induced dyspnoea inevitably impedes its clinical application. Thus, it is urgent to elucidate the mechanism underlying the ZTO-induced dyspnoea. In this study, network pharmacology was firstly performed to search the clue of ZTO-induced dyspnoea. The key target genes of ZTO-induced dyspnoea were analysed using GO enrichment analysis and KEGG pathway analysis. GO analysis suggested that haem binding could be a key molecular function involved in ZTO-induced dyspnoea. Hence, the haemoglobin (Hb) was focused for its oxygen-carrying capacity with haem as its critical component binding to the oxygen. Ultraviolet-visible absorption spectrum indicated that the ZTO injection (ZTOI) perturbed the Soret band of Hb, suggesting an interaction between ZTO and Hb. GC-MS analysis revealed that  $\beta$ -elemene, germacrone, curdione and furanodiene were main components of ZTOI. Molecular docking was used to illustrate the high affinity between representative sesquiterpenes and Hb, which was finally confirmed by surface plasmon resonance, suggesting their potential roles in dyspnoea by ZTO. Following a network pharmacology-driven strategy, our study revealed an intervened Hb-based mechanism underlying the ZTO-induced dyspnoea, providing a reference for elucidating mechanism underlying adverse drug reactions of herbal medicines in clinic.

## KEYWORDS

binding affinity, dyspnoea, haemoglobin, network pharmacology, zedoary turmeric oil

## 1 | INTRODUCTION

Dyspnoea, defined as a subjective experience of breathing discomfort that consists of qualitatively distinct sensations that vary in intensity, is considered as a common, distressing and non-specific symptom of cardiopulmonary and

neuromuscular diseases. This complex symptom warns of a considerable threat impairing life quality, which causes attention worldwide due to the significant and frustrating time and cost in the evaluation for both clinician and patient.<sup>1,2</sup> Not just the dyspnoea manifested in diseases, the dyspnoea induced by medications has also been greatly

This is an open access article under the terms of the Creative Commons Attribution-NonCommercial-NoDerivs License, which permits use and distribution in any medium, provided the original work is properly cited, the use is non-commercial and no modifications or adaptations are made.

© 2022 The Authors. *Basic & Clinical Pharmacology & Toxicology* published by John Wiley & Sons Ltd on behalf of Nordic Association for the Publication of BCPT (former Nordic Pharmacological Society).

concerned. For instance, increasing dyspnoea was characterized in the pulmonary toxicity from taxanes in the chemotherapy regimens for non-small-cell lung cancer. And patients with lung cancer receiving epidermal growth factor receptor-tyrosine kinase inhibitor therapy would present with acute dyspnoea.<sup>3</sup> Besides, it was described that a patient developed dyspnoea after being treated with quetiapine, an atypical antipsychotic.<sup>4</sup> As a typical type of adverse drug reaction, the drug-induced dyspnoea should be paid close attention for its potential leading to mortality.

Zedoary turmeric oil (ZTO) is the volatile oil extracted from the rhizome of *Curcuma phaeocaulis* V al., *Curcuma wenyujin* Y. H. Chen et C. Ling or *Curcuma kwangsiensis* S. G. Lee et C. F. Liang. It has been reported that ZTO has multiple bioactivities, including antitumour, anti-inflammation, antifungus and treatment of psoriasis.<sup>5–8</sup> Clinically, ZTO has been widely used as an injection for its antiviral effect to treat upper respiratory tract infection, children viral pneumonia, digestive tract ulcer, viral hepatitis A and so on.<sup>9</sup> Unfortunately, the occurrence of adverse drug reaction during the application of ZTO has been paid great attention. The common clinical manifestations of ZTO-induced adverse drug reaction are dyspnoea, allergy, rash, nausea, vomiting, palpitation and so on, with dyspnoea as the main symptom. Dyspnoea induced by ZTO often occurs rapidly when ZTO is administered, accompanied by chest distress, cyanosis and even respiratory failure, which becomes a potential life threat during the ZTO-based therapy. However, little is currently known about the biological mechanism underlying the ZTO-induced dyspnoea, which causes a huge obstacle impeding the clinical application of ZTO.

Therefore, we tried to investigate the potential mechanisms underlying the ZTO-associated dyspnoea. As ZTO contains various components with multiple targets, the network pharmacology study which is a powerful approach for dissecting mechanism of complex natural medicine based on the integration of multidirectional pharmacology, computational biology and network analysis was performed.<sup>10</sup> It was indicated by gene ontology (GO) enrichment analysis that the haem binding could be the potential mechanism underlying ZTO-induced dyspnoea. Given that the haem is a key component binding to the oxygen carried by haemoglobin (Hb), Hb was resultantly targeted to further study. Associated with clinical application of ZTO, the ZTO injection (ZTOI) was further used to validate whether ZTO interacted with Hb. Ultraviolet (UV)-visible absorption spectrum measurement was applied, and it was observed that both normal ZTOI and abnormal ZTOI (recalled ZTOI which induced dyspnoea in clinic) decreased the peak intensity of Soret band of Hb, suggesting an interaction between ZTO and Hb. The GC-MS was applied to characterize the

chemical composition of ZTOI, and the several sesquiterpenes were identified as the main components of ZTOI. Furthermore, the binding affinity between main sesquiterpenes and Hb were illustrated using molecular docking and finally confirmed by surface plasmon resonance (SPR). Our study suggested that the interaction between ZTO and Hb, a key protein with carrying oxygen as its major physiological function, might be the potential mechanism underlying the dyspnoea induced by ZTO. More importantly, this study provided a reference for elucidating the mechanism underlying the adverse drug reaction of herbal medical products occurred in clinic and a potent foundation for quality control methodology to better ensure the safety of clinical application.

## 2 | MATERIALS AND METHODS

The study was conducted in accordance with the Basic & Clinical Pharmacology & Toxicology policy for experimental and clinical studies.<sup>11</sup>

### 2.1 | Chemicals and reagents

Normal and abnormal ZTOI were provided by the manufacturer. The standard compounds of  $\beta$ -elemene, germacrone, curdione and furanodiene were purchased from Shanghai Yuanye Bio-Technology Co., Ltd. Human Hb and dimethyl sulphoxide (DMSO) were purchased from Sigma-Aldrich (St. Louis, MO, USA).

### 2.2 | Chemical compounds of ZTO

The information on chemical components in ZTO was obtained from Traditional Chinese Medicine Systems Pharmacology Database and Analysis Platform (TCMSP, <https://old.tcmsp-e.com/tcmsp.php>) and literature retrieved from China National Knowledge Infrastructure (<https://www.cnki.net/>) and PubMed (<https://pubmed.ncbi.nlm.nih.gov/>).

### 2.3 | Prediction of ZTO-related targets

TCMSP, Traditional Chinese Medicines Integrated Database (TCMID, <http://47.100.169.139/tcmid/>) and DrugBank (<https://www.drugbank.com/>) databases were used to retrieve the ZTO-related targets by uploading compound names. The SMILES information of chemical components in ZTO was submitted to SwissTargetPrediction (<http://www.swisstargetprediction.ch/>) to predict potential targets of ZTO.

## 2.4 | Potential dyspnoea-related target genes

The target genes retrieved from Online Mendelian Inheritance in Man (OMIM, <https://omim.org/>), GeneCards (<https://www.genecards.org/>) and Comparative Toxicogenomics Database (CTD, <http://ctdbase.org/>) were merged. Standardization of the gene name and definition of the species as *Homo sapiens* was performed in the UniProt (<https://www.uniprot.org/>) database. The keyword used in the search was “dyspnoea.” The overlapping genes of ZTO and dyspnoea-related targets were considered as the key potential target genes of ZTO-induced dyspnoea.

## 2.5 | Construction of compound-target network

The compound-target network was constructed for the 36 compounds and related gene targets associated with dyspnoea using Cytoscape 3.7.2 (<http://www.cytoscape.org/>). Compounds and target genes were represented by nodes and their interactions were indicated by edges. The network was analysed to calculate values of degree, betweenness centrality (BC) and closeness centrality (CC) which were critical topological parameters suggesting the importance of compounds or targets in the network.

## 2.6 | GO and KEGG enrichment analysis

Metascape (<https://metascape.org/gp/index.html#/main/step1>) was applied for GO function enrichment analysis and KEGG pathway enrichment analysis. The minimal overlap was set as 3, the *p* value cut-off was 0.01, and the minimal enrichment factor was 1.5. The *p* values were calculated based on the accumulative hypergeometric distribution, and *q* values were calculated using the Benjamini–Hochberg procedure to account for multiple testing. The most statistically significant term within a cluster was chosen to represent the cluster and displayed.

## 2.7 | UV-visible absorption spectrum measurement

Hb (0.1 mg/ml, dissolved in phosphate-buffered saline) was treated with 1 mg/ml normal or abnormal ZTOI. After incubation for 10 min at 25°C, the UV-visible absorption spectra were recorded using a microplate reader (SYNERGY H1, BioTek, USA).

## 2.8 | GC-MS analysis

GC-MS analysis was performed using an Agilent 7890A GC System twinned with an Agilent 5975C inert MSD with Triple-Axis Detector. The GC column configuration used comprised an Agilent HP-5MS Ultra Inert (30 m × 250 μm × 0.25 μm) column for chromatographic separation. The injection port was set to 270°C without split mode. Helium was used as carrier gas with constant flow rate of 1.0 ml/min. The oven was initially held at 50°C for 1 min then ramped to 170°C at 10°C/min and to 230°C at 5°C/min. The auxiliary temperature was programmed at 250°C. Liquid injections (1 μl) were achieved using an Agilent 7693 Autosampler. The mass spectrometer high-efficiency EI source was set to 230°C, and quadrupole was set at 150°C. Mass spectra were recorded in full-scan mode ranging from 45–600 amu in positive ion mode after a solvent delay of 3 min. The components of ZTOI were identified using library from the National Institute of Standards and Technology 17.

## 2.9 | Molecular docking

The structure of β-elemene, curdione, germacrone and furanodiene was downloaded from PubChem (<https://pubchem.ncbi.nlm.nih.gov/>) and converted into pdb format using Open Babel 3.1.1. The structure of Hb was downloaded from RCSB Protein Data Bank (PDB ID: 1BBB, <https://www.rcsb.org/structure/1BBB>) as pdb format. The docking was accomplished using AutoDock Tools 1.5.7, in which water was deleted, non-polar hydrogen atoms were added, and electric charges were calculated. A grid box with size of 70 × 60 × 64 Å was set to fix around the Hb. The docked conformations were tabulated according to their binding free energies. The conformation with the highest affinity or hydrogen bonds were further analysed by Discovery Studio 4.5 Client (Discovery Studio 4.5, Accelrys, Co. Ltd) and visualized by PyMOL (version 2.5.2).

## 2.10 | SPR analysis

The interaction of representative sesquiterpenes in ZTOI between Hb was detected using SPR (Biacore T200, GE Healthcare). Hb was dissolved in HBS-N buffer (0.01 M HEPES, pH 7.4, 0.15 M NaCl, GE Healthcare) and diluted to 100 μg/ml with 10 mM acetate (pH 5.5). The amine coupling kit (GE Healthcare) was used to immobilize Hb on a CM5 sensor chip (Series S, Cytiva). According to recommendation of manufacturer, 1-ethyl-3-(3-dimethylaminopropyl)-carbodiimide hydrochloride

**TABLE 1** The target information of zedoary turmeric oil to dyspnoea

Protein name	UniPort ID	Gene name
Sodium channel protein type 5 subunit $\alpha$	Q14524	SCN5A
Prostaglandin G/H synthase 2	P35354	PTGS2
Tumour necrosis factor	P01375	TNF
Interleukin-1 $\beta$	P01584	IL1B
Interleukin-6	P05231	IL6
Nitric oxide synthase, inducible (by homology)	P35228	NOS2
Nitric oxide synthase, endothelial	P29474	NOS3
$\beta$ -2 Adrenergic receptor	P07550	ADRB2
Glucocorticoid receptor	P04150	NR3C1
Apoptosis regulator Bcl-2	P10415	BCL2
Cyclin-dependent kinase inhibitor 1	P38936	CDKN1A
Cellular tumour antigen p53	P04637	TP53
Cytochrome P450 2D6	P10635	CYP2D6
Cytochrome P450 3A4	P08684	CYP3A4
Cytochrome P450 1A2	P05177	CYP1A2
Cytochrome P450 1A1	P04798	CYP1A1
Poly [ADP-ribose] polymerase-1	P09874	PARP1
Haem oxygenase 1 (by homology)	P09601	HMOX1
Caspase-3	P42574	CASP3
Mitogen-activated protein kinase 14	Q16539	MAPK14
Myeloperoxidase	P05164	MPO
Peroxisome proliferator-activated receptor gamma	P37231	PPARG
Pregnane X receptor	O75469	NR1I2
Glycogen synthase kinase-3 $\beta$	P49841	GSK3B
Epidermal growth factor receptor erbB1	P00533	EGFR
MAP kinase ERK2	P28482	MAPK1
Tyrosine-protein kinase JAK2	O60674	JAK2
Arachidonate 5-lipoxygenase	P09917	ALOX5
Nuclear factor erythroid 2-related factor 2	Q16236	NFE2L2
Serine/threonine-protein kinase AKT	P31749	AKT1
Signal transducer and activator of transcription 3	P40763	STAT3

(EDC) and *N*-hydroxysuccinimide (NHS) were used to activate the chip, and residual activated groups were blocked by 1.0 M ethanolamine-HCl (pH 8.5). The

running buffer was 1.05 $\times$  PBS-P containing 5% DMSO (v/v) and 0.02% surfactant P20 (v/v). Each sesquiterpene was accurately weighed and dissolved in DMSO to prepare stock solutions. The sensorgrams were fitted by the 1:1 binding model to calculate equilibrium dissociation constant (KD) in Biacore T200 Evaluation Software (version 3.2, General Electric Company).

## 2.11 | Statistics

Data are presented as means  $\pm$  standard deviation. The data distribution and homogeneity of variances were firstly analysed by Shapiro–Wilk and Bartlett's tests, respectively. Means between groups were compared using one-way analysis of variance (ANOVA) where appropriate, and Tukey's post hoc test was used. All analyses and graphical presentation were performed using GraphPad Prism 8 software (GraphPad Software, La Jolla, CA, USA).  $p < 0.05$  was considered as statistically significant.

## 3 | RESULTS

### 3.1 | Compound-target network

A total of 36 components in ZTO were finally included for target prediction, many of which were monoterpenoids or sesquiterpenes (Table S1). And 242 gene candidates related to ZTO bioactivity and 266 gene targets associated with dyspnoea were obtained from multiple databases. The Venn diagram suggested that 31 common targets of both ZTO and dyspnoea were considered as critical potential targets of ZTO-related dyspnoea (Table 1 and Figure 1). Thus, these 31 target genes were used for compound-target network construction and further analysis. The compound-target network included 67 nodes (36 compound nodes and 31 target nodes) and 79 edges (Figure 1). Notably, the network contained several compounds with higher values of degree, BC and CC, which suggested their essential roles in the network, for example, demethoxycurcumin, ar-turmerone, reynosin, camphor,  $\beta$ -elemene and furanodiene.

### 3.2 | GO and KEGG enrichment analysis

The Metascape was used to unveil the gene function annotation of the selected 31 target genes. In total, 1038 entries of biological processes, 30 entries of cellular components and 44 entries of molecular functions were

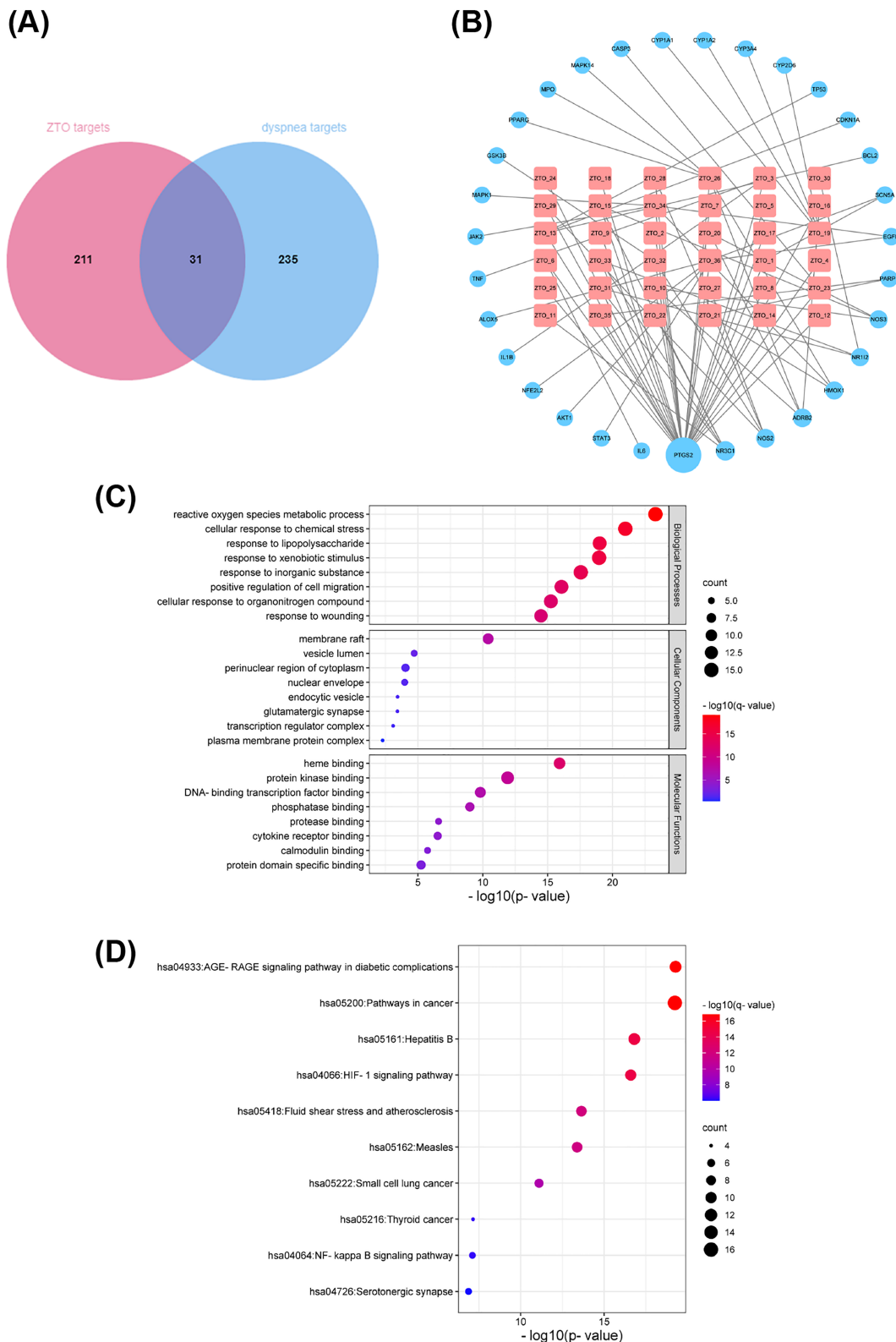


**FIGURE 1** The network pharmacology study of dyspnoea induced by zedoary turmeric oil (ZTO). (A) Venn diagram of the overlapping targets in ZTO and dyspnoea. (B) Compound-target network diagram. The pink round rectangles represent the compounds in ZTO. The light blue circles represent the common target genes of ZTO and dyspnoea. Node size was proportional to the value of degree. (C) Gene ontology (GO) enrichment analysis. Bubble size represents the number of genes involved in the GO enrichment. Colour represents the adjusted  $p$  value in log base 10. (D) KEGG pathway enrichment analysis. Bubble size represents the number of genes enriched in pathways. Colour represents the adjusted  $p$  value in log base 10

obtained. It was demonstrated in GO enrichment analysis that the main biological processes involved in the ZTO-induced dyspnoea were reactive oxygen species metabolic process (GO:0072593), cellular response to chemical stress (GO:0062197), response to xenobiotic stimulus (GO:0009410), response to inorganic substance (GO:0010035), response to lipopolysaccharide (GO:0032496), positive regulation of cell migration (GO:0030335), cellular response to organonitrogen compound (GO:0071417) and response to wounding (GO:0009611). The enrichment of cellular components indicated that these processes occurred mainly in the membrane raft (GO:0045121), perinuclear region of cytoplasm (GO:0048471), vesicle lumen (GO:0031983), nuclear envelope (GO:0005635), endocytic vesicle (GO:0030139), glutamatergic synapse (GO:0098978), transcription regulator complex (GO:0005667) and plasma membrane protein complex (GO:0098797). The following molecular functions were strongly connected with ZTO-related dyspnoea, including haem binding (GO:0020037), protein kinase binding (GO:0019901), DNA-binding transcription factor binding (GO:0140297), phosphatase binding (GO:0019902), protein domain specific binding (GO:0019904), cytokine receptor binding (GO:0005126), protease binding (GO:0002020) and calmodulin binding (GO:0005516) (Figure 1). The relationship between target genes and important pathways was elucidated by KEGG pathway enrichment analysis. It was discovered that 31 target genes were enriched in 118 signalling pathways, mainly involving AGE-RAGE signalling pathway in diabetic complications (hsa04933), pathways in cancer (hsa05200), hepatitis B (hsa05161), HIF-1 signalling pathway (hsa04066), fluid shear stress and atherosclerosis (hsa05418), measles (hsa05162), small-cell lung cancer (hsa05222), NF-kappa B signalling pathway (hsa04064), serotonergic synapse (hsa04726) and thyroid cancer (hsa05216) (Figure 1).

### 3.3 | ZTOI decreased the peak intensity of Soret band of Hb

As indicated by the GO enrichment analysis that the haem binding was strongly involved in the ZTO-related dyspnoea, we decided to investigate the interaction between ZTO and Hb which is a key protein mainly responsible for carrying oxygen, with haem as the key component binding to the oxygen. Notably, it has been reported that the disturbed Hb could be strongly associated with the occurrence of dyspnoea in clinic, which provides a potential clue to understand the mechanisms underlying the ZTO-induced dyspnoea.<sup>12</sup> And UV-visible absorption measurement is an effective approach to

investigate the structure change of protein and to understand the ligand-protein complex formation. It is well known that Hb has several characteristic absorption peaks. The strong absorption peak at 406 nm corresponds to porphyrin-Soret band generated from haem.<sup>13,14</sup> The change of UV-visible absorption spectrum of Hb provided important information for conformation change of protein and ligand-protein interaction. To be associated with clinical practice, ZTOI, the pharmaceutical products in clinic of ZTO, was used to investigate the interactions between ZTO and Hb. It was shown that compared with the Hb, the addition of normal or abnormal ZTOI caused a decreased peak intensity of Soret band, respectively, among which the abnormal ZTOI exhibited more remarkable effect. And the shape of peak was prone to change into a non-Gaussian shape with the treatment of abnormal ZTOI (Figure 2). Consistently, the optical density (OD) values at 406 nm (the wavelength in which Soret band reached the highest peak intensity in our study) of Hb treated with normal or abnormal ZTOI were apparently lower than that of Hb alone (Figure 2). Besides, the characteristic band of Hb is also located at 280 nm due to the phenyl group of tryptophan and tyrosine residues. Further, it was observed that the bands of Hb treated with normal or abnormal ZTOI at around 280 nm were affected, which was suggestive of the presence of effective interactions between the aromatic residues and the ZTOI. Therefore, our study suggested that the dyspnoea induced by ZTO in clinic might be associated with interaction between Hb and ZTO.

### 3.4 | Chemical composition identification of ZTOI by GC-MS

We moved on to investigate the compounds in the ZTOI that might interact with Hb. Thus, GC-MS was firstly applied to analyse the chemical compositions of ZTOI. Several monoterpenes were firstly separated and identified in ZTOI, including eucalyptol, linalool and (–)-camphor. More importantly, it was then discovered that  $\beta$ -elemene, curzerene,  $\beta$ -elemenone, germacrone and curdione were identified with more abundant contents (Figure 3 and Table 2). Although the curzerene had the highest peak area suggested by GC-MS analysis, it was reported that the curzerene could be transformed from furanodiene during GC-MS analysis, in which high temperature was required for the gasification of analytes.<sup>15</sup> Besides, furanodiene was highlighted in our compound-target network, and it is also the key indicator used in the content determination of ZTO using high-performance liquid chromatography according to the Chinese pharmacopoeia.<sup>16</sup> More importantly, it has been

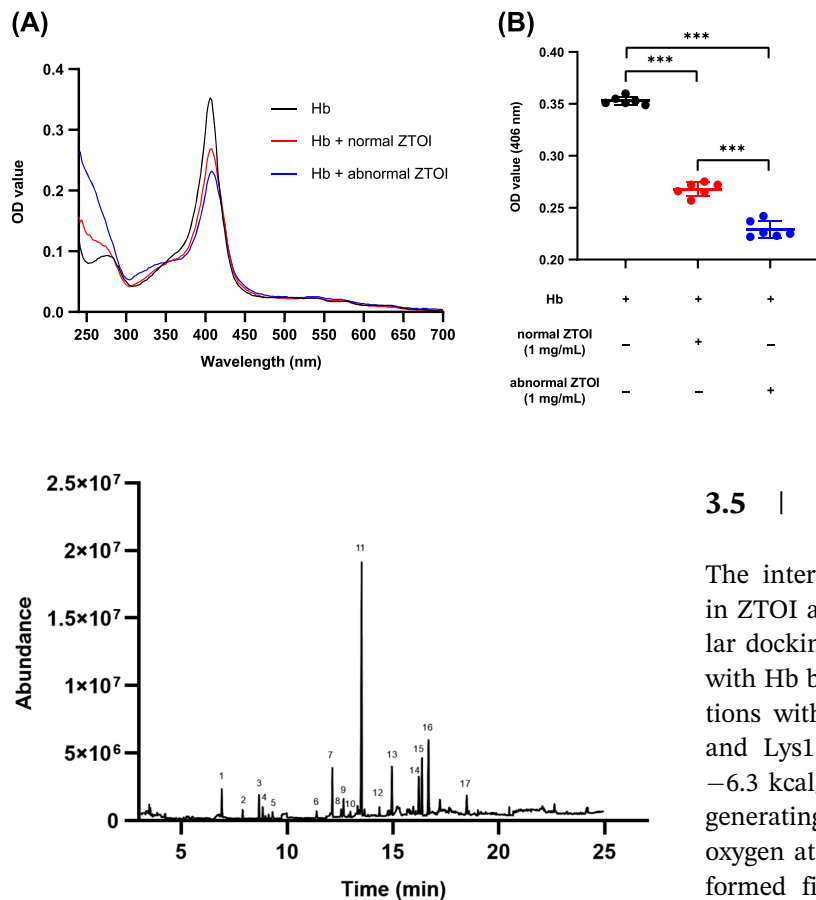


**FIGURE 2** Ultraviolet-visible absorption spectrum determination. (A) The ultraviolet-visible absorption spectrum of haemoglobin (Hb) treated with normal or abnormal zedoary turmeric oil injection (ZTOI, 1 mg/ml). OD, optical density. (B) The absorbance at 406 nm of Hb treated with normal or abnormal ZTOI. \*\*\*  $p < 0.001$

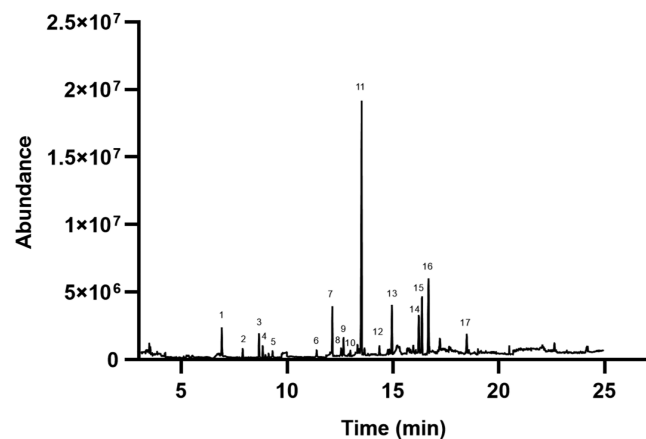


**FIGURE 3** Total ion chromatography of zedoary turmeric oil injection by GC-MS. Partial monoterpenes and sesquiterpenes were identified, including (1) eucalyptol, (2) linalool, (3) (-)-camphor, (4) isoborneol, (5) (+)- $\alpha$ -terpineol, (6)  $\delta$ -elemene, (7)  $\beta$ -elemene, (8) caryophyllene, (9)  $\gamma$ -elemene, (10) humulene, (11) curzerene, (12) germacrene B, (13)  $\beta$ -elemenone, (14) neocurdione, (15) germacrone, (16) curdione and (17) curcumenone

reported that furanodiene inhibits breast cancer cell growth via altering mitochondrial function in an AMP-activated protein kinase-dependent manner.<sup>17</sup> Thus, furanodiene was proceeded to further study instead of curzerene.  $\beta$ -Elemene, a well-known sesquiterpene, is known for its inhibitory effect on multiple carcinomas.<sup>18</sup> Germacrone and curdione are also paid close attention for their therapeutic effects on different types of cancers, like prostate cancer, oesophageal squamous cell carcinoma and uterine leiomyosarcoma.<sup>19–21</sup> Besides, germacrone and curdione are also detected in the pharmacokinetic study of ZTO.<sup>22,23</sup> Therefore,  $\beta$ -elemene, furanodiene, germacrone and curdione were considered as the representative components in ZTOI and selected to further study.  $\beta$ -Elemenone was abolished due to the unavailability of standard compound.

### 3.5 | Molecular docking

The interactions between representative sesquiterpenes in ZTOI and Hb were firstly explored by virtual molecular docking using AutoDock Vina.  $\beta$ -Elemene interacted with Hb by forming alkyl or  $\pi$ -alkyl hydrophobic interactions with Tyr35, Pro36, Trp37, Pro95, Lys127, Ala130 and Lys139, with an estimated Gibb's free energy of  $-6.3$  kcal/mol. Furanodiene bound strongly with Hb by generating one conventional hydrogen bond between oxygen atom on its furan ring and Lys139 of Hb. It also formed five alkyl or  $\pi$ -alkyl hydrophobic interactions with Val33, Pro36, Pro51, Val 54 and Ala123. The Gibb's free energy of furanodiene-Hb interaction was predicted to be  $-6.9$  kcal/mol. The carbonyl group of germacrone formed one conventional hydrogen bond with Arg104 of Hb, and the complex was stabilized by other four alkyl or  $\pi$ -alkyl hydrophobic interactions with Phe36, Leu100, Ala135 and Tyr145. The Gibb's free energy of germacrone-Hb interaction was estimated to be  $-7.0$  kcal/mol. The curdione-Hb complex was generated by forming two conventional hydrogen bonds among the carbonyl group at C-4 of curdione and Val1 or Ser138 of Hb and stabilized by four alkyl or  $\pi$ -alkyl hydrophobic interactions with Trp37, Pro95, Lys127 and Ala130, with predicted free energy of  $-6.9$  kcal/mol (Figure 4).

### 3.6 | The validation of binding of representative sesquiterpenes in ZTOI to Hb by SPR

The interactions between representative sesquiterpenes in ZTOI and Hb were further validated by SPR, one of the most prominent optical biosensor technologies in analysing real-time biomolecular interaction.<sup>24</sup> The acetate buffer at pH 5.5 was used, because it generated the highest response of Hb (Figure S1). The binding reaction was characterized by injections of sesquiterpenes at

TABLE 2 The identification of compounds in zedoary turmeric oil injection

Peak No.	Compounds	Formula	Molecular weight	$t_R$ (min)	Ion information (m/z)
1	Eucalyptol	C <sub>10</sub> H <sub>18</sub> O	154.25	6.914	111.1798, 108.1894, 84.1720, 81.1999, 71.1693
2	Linalool	C <sub>10</sub> H <sub>18</sub> O	154.25	7.904	93.1877, 71.1999, 69.1508, 55.1493
3	(-)-Camphor	C <sub>10</sub> H <sub>16</sub> O	152.23	8.677	108.1420, 95.1999, 81.1620, 69.1290
4	Isoborneol	C <sub>10</sub> H <sub>18</sub> O	154.25	8.851	121.1140, 110.0161, 95.1999, 93.1187
5	(+)- $\alpha$ -Terpineol	C <sub>10</sub> H <sub>18</sub> O	154.25	9.315	136.1744, 121.1827, 93.1892, 81.1528, 59.1999
6	$\delta$ -Elemene	C <sub>15</sub> H <sub>24</sub>	204.35	11.396	136.1605, 121.1999, 93.1656, 91.1276
7	$\beta$ -Elemene	C <sub>15</sub> H <sub>24</sub>	204.35	12.138	107.1682, 93.1999, 81.1872, 67.1573
8	Caryophyllene	C <sub>15</sub> H <sub>24</sub>	204.35	12.556	133.1901, 93.1999, 91.1800, 79.0630, 69.1629
9	$\gamma$ -Elemene	C <sub>15</sub> H <sub>24</sub>	204.35	12.669	121.1999, 107.1436, 93.1607
10	Humulene	C <sub>15</sub> H <sub>24</sub>	204.35	12.991	121.1299, 93.1999, 92.1185, 80.1335
11	Curzerene	C <sub>15</sub> H <sub>20</sub> O	216.32	13.527	148.1407, 108.1999, 91.1149, 79.1143
12	Germacrene B	C <sub>15</sub> H <sub>24</sub>	204.35	14.365	121.1999, 119.1439, 107.1532, 105.1578, 93.1664
13	$\beta$ -Elemenone	C <sub>15</sub> H <sub>22</sub> O	218.33	14.958	135.1875, 121.1800, 107.1999, 93.1392, 91.1329, 67.1332
14	Neocurdione	C <sub>15</sub> H <sub>24</sub> O <sub>2</sub>	236.35	16.225	180.1999, 167.1943, 109.1549, 69.0541, 68.1259, 55.1259
15	Germacrone	C <sub>15</sub> H <sub>22</sub> O	218.33	16.376	136.1605, 135.1798, 107.1999, 67.1421
16	Curdione	C <sub>15</sub> H <sub>24</sub> O <sub>2</sub>	236.35	16.685	180.1999, 167.1840, 109.1824, 69.1816, 55.1438
17	Curcumenone	C <sub>15</sub> H <sub>22</sub> O <sub>2</sub>	234.34	18.488	176.1999, 161.1710, 149.1702, 68.1672, 67.1512

different concentrations over the Hb immobilized on the biosensor chip surface. In total, 9138.1 response unit of Hb was immobilized (Figure S2). Germacrone, furanodiene, curdione and  $\beta$ -elemene all exhibited kinetic binding characteristics when interacting with Hb. Fitted by 1:1 binding model, the KD values of germacrone and furanodiene were  $7.540 \times 10^{-5}$  M and  $1.825 \times 10^{-5}$  M, respectively. Furthermore, curdione and  $\beta$ -elemene showed higher affinity to Hb, with their KD values to be  $3.795 \times 10^{-6}$  M and  $2.272 \times 10^{-6}$  M, respectively (Figure 5). Thus, these representative sesquiterpenes in ZTOI showed high binding affinity to Hb, which might be the potential substances in ZTO inducing dyspnoea.

## 4 | DISCUSSION

Dyspnoea, considered as a subjective experience of breathing discomfort that consists of qualitatively distinct sensations of varying intensity, is also a common type of adverse drug reaction causing an unpleasant clinical outcome.<sup>25</sup> Due to the excellent antiviral bioactivity, the application of ZTO in clinic has been paid close attention, which, however, is impeded by the frustrating induced dyspnoea. Therefore, it is of great importance to understand the potential biological process behind the ZTO-induced dyspnoea, which would be helpful for safer usage of ZTO in clinic.

Network pharmacology is an interdisciplinary approach based on artificial intelligence and big data, characterized by its systematic nature, relevance and predictability, which was firstly performed to explore the clue of ZTO-induced dyspnoea in our study.<sup>26</sup> The compound-target network revealed some key components in ZTO strongly involved in dyspnoea with higher values of degree, BC and CC, including demethoxycurcumin, ar-turmerone, reynosin, camphor,  $\beta$ -elemene and furanodiene. Among them,  $\beta$ -elemene, a typical sesquiterpene in ZTO, has aroused interest worldwide by exhibiting potent therapeutic effects on treatment of multiple carcinomas, including hepatocarcinoma, glioblastoma, non-small-cell lung cancer and cervical cancer.<sup>27</sup> However, dyspnoea and cyanosis induced by  $\beta$ -elemene, the similar adverse drug reactions to ZTO, are observed when  $\beta$ -elemene was administered in clinic. For example, the intrapleural injection of elemene to the patients suffering from malignant pleural effusion induced dyspnoea, accompanied with cyanosis, severe chest pain and wheezing. Apart from dyspnoea, it was reported that fever, phlebitis and liver dysfunction also occurred when  $\beta$ -elemene was administered as well as some gastric abnormalities.<sup>28</sup> Camphor is a cyclic monoterpene originally discovered in the wood of the camphor laurel (*Cinnamomum camphora*) which is famous for its local anaesthetic effect. Nevertheless, it is concerned for its neurotoxicity and hepatotoxicity due to the degenerative and necrotic



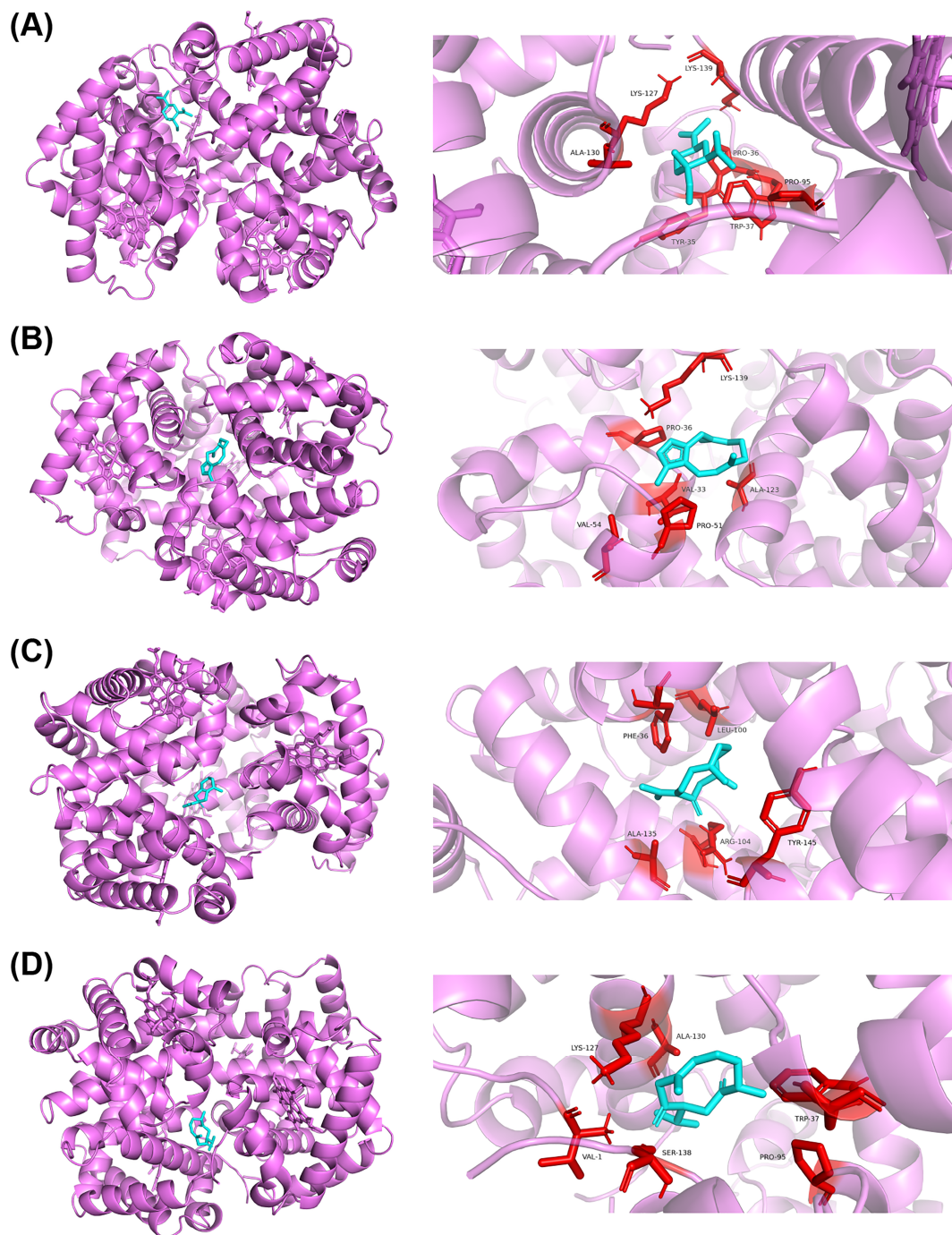
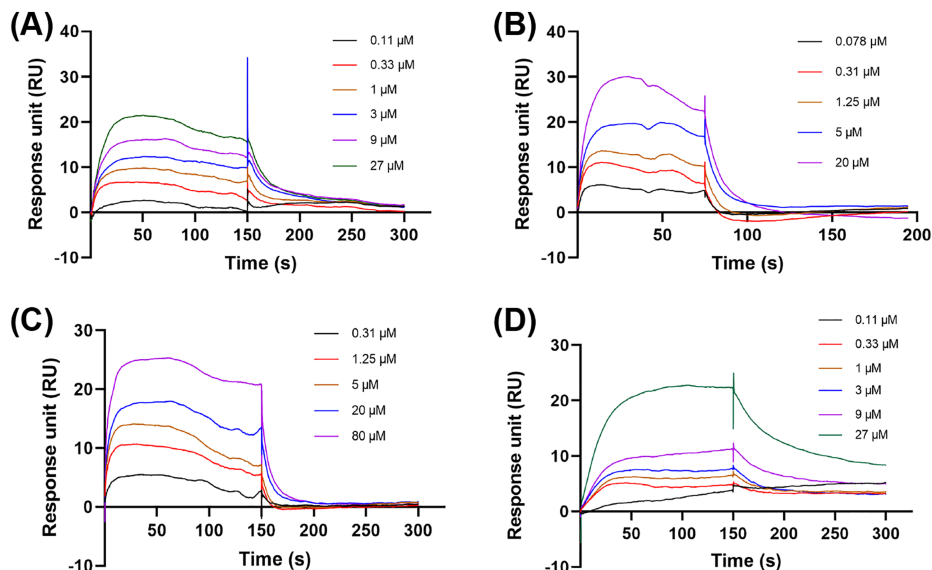


**FIGURE 4** Molecular docking of different compounds with haemoglobin. (A)  $\beta$ -Elemene, (B) furanodiene, (C) germacrone and (D) curdione

changes in the central nervous system and massive hepatocellular damage after chronic oral exposure to camphor.<sup>29</sup> And the relationship among neurodevelopmental disorders, liver disease and hypoxia or hypoxia inducible factor signalling pathway which is enriched by KEGG pathway analysis in our study has been extensively discussed, leading to a potential clue of ZTO compound-related tissue hypoxia.<sup>30,31</sup> Hence,  $\beta$ -elemene or camphor should be focused for their potential roles in ZTO-

induced dyspnoea and considered in the quality control methodology for ZTO. Apart from some key compounds, some potential targets were also highlighted by network pharmacology study. The compound-target network suggested that PTGS2 had a high value of Degree, suggesting its potential role in ZTO-induced dyspnoea. It has been reported that the expression of prostaglandin H synthase 2 in cytotrophoblasts isolated from term placentas was up-regulated in the hypoxic atmosphere and

**FIGURE 5** Surface plasmon resonance sensorgrams of different compounds with haemoglobin. (A)  $\beta$ -Elemene, (B) furanodiene, (C) germacrone and (D) curdione



its enzyme activity, indicated by increased prostaglandin E2 and thromboxane release.<sup>32</sup> Besides, the reactive oxygen species metabolism was highlighted in the GO enrichment analysis as a key biological process. It was demonstrated that the elevated reactive oxygen species could cause diaphragm muscle weakness, which might deteriorate breathing abnormalities, exercise intolerance and dyspnoea.<sup>33</sup> It was also revealed that the reactive oxygen species evoked by mitochondrial dysfunction caused nociceptor hyperexcitability, which is associated with airway sensory nerve excitability, a key determinant of respiratory disease-associated reflexes and sensations such as cough and dyspnoea.<sup>34</sup> These potential relationships expand the idea in exploring the mechanism underlying ZTO or other drug-induced dyspnoea. Therefore, importantly, the advantage of network pharmacology-driven strategy could be emphasized for the rapid screening of candidate components which might be the risk factor inducing adverse drug action to enhance the pertinence of quality control for the safer clinical drug use.

As indicated by the GO enrichment analysis, the haem binding might be a critical molecular function strongly involved in ZTO-related dyspnoea. Therefore, Hb was targeted for further analysis. It is well known that Hb is a tetramer consisting of two  $\alpha$ -subunits and two  $\beta$ -subunits, and each subunit has a binding pocket for haem which consists of a ferrous ion in the centre of porphyrin and coordinated by the four nitrogen atoms of porphyrin ring. The ferrous ion is covalently anchored to Hb at the haem pocket by an imidazole of the histidine residue, which allows the ferrous ion to bind to the oxygen, giving Hb the function of carrying oxygen.<sup>35,36</sup> It is discovered that the strong Soret band at about 406 nm in

the UV-visible absorption spectrum of Hb originates from the haem group, of which shape, position and intensity can provide critical information about the possible interactions. It was demonstrated in our study that the treatment of either normal or abnormal ZTOI decreased the peak intensity of Soret band and a trend of peak shape changing into a non-Gaussian shape was observed with the treatment of ZTOI by using UV-visible absorption spectrum measurement, suggesting an interaction between ZTOI and oxygen binding domain of Hb. Notably, it was reported that the transition to non-Gaussian shape of the Soret band indicated the location move of the iron atom from the in-plane toward the out-of-haem plane, which generates a conformational heterogeneity.<sup>13</sup> Thus, our study suggested a potential perturbation on the structure of haem by ZTOI. Importantly, it was noticed that the patients with structural mutation in Hb were suffering from a decreased oxygen affinity, with clinical manifestation as dyspnoea, lower oxygen saturation, cyanosis and tissue hypoxia.<sup>12,37,38</sup> Thus, a disturbed Hb-based mechanism was proposed to elucidate the ZTO-induced dyspnoea. Additionally, there are other cases of drug-induced dyspnoea which are related to the perturbed Hb. For instance, a patient with nephrotic syndrome presented with shortness of breath after administration of dapsone which was considered as the cause of methaemoglobinaemia by oxidating  $\text{Fe}^{2+}$ .<sup>39</sup> Therefore, it is speculated that Hb would be a critical target strongly associated with the drug-induced dyspnoea.

Moreover, our study focuses on the main compounds in ZTO. However, as a medical product applied in clinic, the potential role of excipients in ZTOI in inducing dyspnoea should be also considered. In the production of ZTOI, Tween 80 is largely used as the excipient to improve

the solubility of ZTO. In our study, the effect of ZTO on the Hb was designed using both normal and abnormal ZTOI which had the same concentration of Tween 80. Although the main sesquiterpenes in the ZTOI, including  $\beta$ -elemene, furanodiene, germacrone and curdione, were highlighted with responsibilities to the dyspnoea induced by ZTO, the potential role of Tween 80 in inducing adverse drug reactions cannot be ignored. Notably, it has been reported that Tween 80 plays a critical role in the onset of dyspnoea or other adverse drug reactions, like anaphylactoid reaction, suggesting its role as a risk factor inducing adverse drug reaction.<sup>40,41</sup> Unfortunately, the content of Tween 80 is less concerned in the quality control of ZTOI. Therefore, it is critical that the quality control of ZTOI should be optimized with the consideration of suitable content of Tween 80, and it is meaningful to clarify the potential role of Tween 80 in the pathogenesis of dyspnoea or other adverse drug reactions.

In our study, the interaction between ZTO and Hb was tested in vitro. Thus, an in vivo study is encouraged for the in-depth elucidation of the relationships among ZTO, Hb and dyspnoea. For example, the dose-toxic effect of ZTO should be further investigated, which might be helpful for avoiding the onset of ZTO adverse drug reactions. Generally, our study revealed an intervened Hb-based mechanism, which might be helpful for understanding biological processes of dyspnoea induced by other medical products. Meanwhile, this proposed mechanism would also be a useful basis for quality control methodology to better ensure the clinical safety of herbal medical products.

## ACKNOWLEDGEMENTS

This work was supported by the National Natural Science Foundation of China (Grants 81773891 and 82130112), the National Key R&D Program of China (Grant 2020YFF01014606) and the Beijing Excellent Talent Project (Grants DFL20190702 and 2018000021223TD09).

## CONFLICT OF INTEREST

The authors declare no competing interests.

## ORCID

Dan Yan  <https://orcid.org/0000-0002-1288-4144>

## REFERENCES

- Parshall MB, Schwartzstein RM, Adams L, et al. An official American Thoracic Society statement: update on the mechanisms, assessment, and management of dyspnea. *Am J Respir Crit Care Med.* 2012;185(4):435-452. doi:10.1164/rccm.201111-2042ST
- Ryan JJ, Waxman AB. The dyspnea clinic. *Circulation.* 2018;137(19):1994-1996. doi:10.1161/CIRCULATIONAHA.117.029769
- Long K, Suresh K. Pulmonary toxicity of systemic lung cancer therapy. *Respirology.* 2020;25(Suppl 2):72-79. doi:10.1111/resp.13915
- Mutschler J, Obermann C, Grosshans M. Quetiapine-induced hyperventilation and dyspnea. *Clin Neuropharmacol.* 2010;33(4):214. doi:10.1097/WNF.0b013e3181e1cc51
- Shi HL, Tan B, Ji G, et al. Zedoary oil (*Ezhu You*) inhibits proliferation of AGS cells. *Chin Med.* 2013;8(1):8. doi:10.1186/1749-8546-8-13
- Su JY, Tan LR, Lai P, et al. Experimental study on anti-inflammatory activity of a TCM recipe consisting of the supercritical fluid CO<sub>2</sub> extract of *Chrysanthemum indicum*, Patchouli Oil and Zedoary Turmeric Oil in vivo. *J Ethnopharmacol.* 2012;141(2):608-614. doi:10.1016/j.jep.2011.08.055
- Wang B, Liu F, Li Q, et al. Antifungal activity of zedoary turmeric oil against *Phytophthora capsici* through damaging cell membrane. *Pestic Biochem Physiol.* 2019;159:59-67. doi:10.1016/j.pestbp.2019.05.014
- Chen J, Ma YQ, Tao YY, et al. Formulation and evaluation of a topical liposomal gel containing a combination of zedoary turmeric oil and tretinoin for psoriasis activity. *J Liposome Res.* 2021;31(2):130-144. doi:10.1080/08982104.2020.1748646
- Li L, Xie Q, Bian G, et al. Anti-H1N1 viral activity of three main active ingredients from zedoary oil. *Fitoterapia.* 2020;142:104489. doi:10.1016/j.fitote.2020.104489
- Zhang SQ, Lai XX, Wang X, et al. Deciphering the pharmacological mechanisms of Guizhi-Fuling capsule on primary dysmenorrhea through network pharmacology. *Front Pharmacol.* 2021;12:613104. doi:10.3389/fphar.2021.613104
- Tveden-Nyborg P, Bergmann TK, Jessen N, Simonsen U, Lykkesfeldt J. BCPT policy for experimental and clinical studies. *Basic Clin Pharmacol Toxicol.* 2021;128(1):4-8. doi:10.1111/bcpt.13492
- Pedroso GA, Fernandes P, Jorge SEDC, et al. Hemoglobin Kirklareli [A<sub>2</sub> 59(E7) His>Leu; HBA2:c.176A>T] in a Brazilian child with severe dyspnea and low O<sub>2</sub> saturation. *Ann Hematol.* 2019;98(12):2853-2855. doi:10.1007/s00277-019-03839-z
- Mahato M, Pal P, Kamilya T, Sarkar R, Chaudhuri A, Talapatra GB. Hemoglobin-silver interaction and bioconjugate formation: a spectroscopic study. *J Phys Chem B.* 2010;114(20):7062-7070. doi:10.1021/jp100188s
- Lykkegaard MK, Ehlerding A, Hvelplund P, et al. A Soret marker band for four-coordinate ferric heme proteins from absorption spectra of isolated Fe(III)-heme<sup>+</sup> and Fe(III)-heme<sup>+</sup> vacuo. *J Am Chem Soc.* 2008;130(36):11856-11857. doi:10.1021/ja803460c
- Yang FQ, Li SP, Zhao J, Lao SC, Wang YT. Optimization of GC-MS conditions based on resolution and stability of analytes for simultaneous determination of nine sesquiterpenoids in three species of *Curcuma* rhizomes. *J Pharm Biomed Anal.* 2007;43(1):73-82. doi:10.1016/j.jpba.2006.06.014
- State Pharmacopoeia Committee. *Pharmacopoeia of the Peoples Republic of China Part I.* China Medical Science Press; 2020.
- Zhong ZF, Tan W, Qiang WW, et al. Furanodiene alters mitochondrial function in doxorubicin-resistant MCF-7 human breast cancer cells in an AMPK-dependent manner. *Mol Biosyst.* 2016;12(5):1626-1637. doi:10.1039/C6MB00003G

18. Qureshi MZ, Attar R, Romero MA, et al. Regulation of signaling pathways by  $\beta$ -elemene in cancer progression and metastasis. *J Cell Biochem.* 2019;120(8):12091-12100. doi:10.1002/jcb.28624
19. Yu ZQ, Xu JP, Shao MF, Zou J. Germacrone induces apoptosis as well as protective autophagy in human prostate cancer cells. *Cancer Manag Res.* 2020;12:4009-4016. doi:10.2147/CMAR.S250522
20. Zhang R, Hao J, Guo KW, et al. Germacrone inhibits cell proliferation and induces apoptosis in human esophageal squamous cell carcinoma cells. *Biomed Res Int.* 2020;2020:7643248. doi:10.1155/2020/7643248
21. Wei C, Li DH, Liu Y, Wang W, Qiu T. Curdione induces antiproliferation effect on human uterine leiomyosarcoma via targeting IDO1. *Front Oncol.* 2021;11:637024. doi:10.3389/fonc.2021.637024
22. You J, Cui FD, Li QP, Yong-sheng W, Han X, Yu YW. A HPLC method for the analysis of germacrone in rabbit plasma and its application to a pharmacokinetic study of germacrone after administration of zedoary turmeric oil. *J Chromatogr B Analyt Technol Biomed Life Sci.* 2005;823(2):172-176. doi:10.1016/j.jchromb.2005.06.032
23. Peng Y, Zhang M, Li WW, et al. A validated LC-MS/MS assay for the quantitative determination of curdione in rabbit plasma and its application to a pharmacokinetic study after administration of zedoary turmeric oil and bioavailability of the oil. *Biomed Chromatogr.* 2014;28(10):1360-1365. doi:10.1002/bmc.3175
24. Oлару A, Bala C, Jaffrezic-Renault N, Aboul-Enein HY. Surface plasmon resonance (SPR) biosensors in pharmaceutical analysis. *Crit Rev Anal Chem.* 2015;45(2):97-105. doi:10.1080/10408347.2014.881250
25. Boyden JY, Connor SR, Otolorin L, et al. Nebulized medications for the treatment of dyspnea: a literature review. *J Aerosol Med Pulm Drug Deliv.* 2015;28(1):1-19. doi:10.1089/jamp.2014.1136
26. An WR, Huang YQ, Chen SQ, et al. Mechanisms of Rhizoma Coptidis against type 2 diabetes mellitus explored by network pharmacology combined with molecular docking and experimental validation. *Sci Rep.* 2021;11(1):20849. doi:10.1038/s41598-021-00293-8
27. Zhai BT, Zhang NN, Han XM, et al. Molecular targets of  $\beta$ -elemene, a herbal extract used in traditional Chinese medicine, and its potential role in cancer therapy: a review. *Biomed Pharmacother.* 2019;114:108812. doi:10.1016/j.biopha.2019.108812
28. Wang B, Peng XX, Sun R, et al. Systematic review of  $\beta$ -elemene injection as adjunctive treatment for lung cancer. *Chin J Integr Med.* 2012;18(11):813-823. doi:10.1007/s11655-012-1271-9
29. Zárbybnický T, Boušová I, Ambrož M, Skálová L. Hepatotoxicity of monoterpenes and sesquiterpenes. *Arch Toxicol.* 2018; 92(1):1-13. doi:10.1007/s00204-017-2062-2
30. Bonkowsky JL, Son J-H. Hypoxia and connectivity in the developing vertebrate nervous system. *Dis Model Mech.* 2018; 11(12):dmm037127. doi:10.1242/dmm.037127
31. Nath B, Szabo G. Hypoxia and hypoxia inducible factors: diverse roles in liver diseases. *Hepatology.* 2012;55(2):622-633. doi:10.1002/hep.25497
32. Nelson DM, Johnson RD, Smith SD, Anteby EY, Sadovsky Y. Hypoxia limits differentiation and up-regulates expression and activity of prostaglandin H synthase 2 in cultured trophoblast from term human placenta. *Am J Obstet Gynecol.* 1999;180(4): 896-902. doi:10.1016/S0002-9378(99)70661-7
33. Laitano O, Ahn B, Patel N, et al. Pharmacological targeting of mitochondrial reactive oxygen species counteracts diaphragm weakness in chronic heart failure. *J Appl Physiol (1985).* 2016; 120(7):733-742. doi:10.1152/jappphysiol.00822.2015
34. Hadley SH, Bahia PK, Taylor-Clark TE. Sensory nerve terminal mitochondrial dysfunction induces hyperexcitability in airway nociceptors via protein kinase C. *Mol Pharmacol.* 2014; 85(6):839-848. doi:10.1124/mol.113.091272
35. Gell DA. Structure and function of haemoglobins. *Blood Cells Mol Dis.* 2018;70:13-42. doi:10.1016/j.bcmd.2017.10.006
36. Ahmed MH, Ghatge MS, Safo MK. Hemoglobin: structure, function and allostery. *Subcell Biochem.* 2020;94:345-382. doi: 10.1007/978-3-030-41769-7\_14
37. Abdulmalik O, Safo MK, Lerner NB, et al. Characterization of hemoglobin bassett ( $\alpha$ 94Asp $\rightarrow$ Ala), a variant with very low oxygen affinity. *Am J Hematol.* 2004;77(3):268-276. doi:10.1002/ajh.20184
38. Barberio G, Leone D, Ivaldi G, et al. Hb Treviso [ $\alpha$ 91(FG3) Leu $\rightarrow$ Phe ( $\alpha$ 2)]: a new slightly unstable hemoglobin variant with moderately decreased oxygen affinity. *Hemoglobin.* 2013; 37(2):107-111.
39. Mannemuddhu SS, Ali R, Kadhemi S, Ruchi R. Unusual cause of persistent dyspnea in a patient with nephrotic syndrome: dapson-induced methemoglobinemia. *CEN Case Rep.* 2021; 10(3):336-340. doi:10.1007/s13730-020-00565-8
40. Bibera MAT, Lo KMK, Steele A. Potential cross-reactivity of polysorbate 80 and cremophor: a case report. *J Oncol Pharm Pract.* 2020;26(5):1279-1281. doi:10.1177/1078155219896848
41. Yang R, Lao QC, Yu HP, et al. Tween-80 and impurity induce anaphylactoid reaction in zebrafish. *J Appl Toxicol.* 2015;35(3): 295-301. doi:10.1002/jat.3069

## SUPPORTING INFORMATION

Additional supporting information may be found in the online version of the article at the publisher's website.

**How to cite this article:** Yang Z, Wang Z, Li J, Long J, Peng C, Yan D. Network pharmacology-based dissection of the underlying mechanisms of dyspnoea induced by zedoary turmeric oil. *Basic Clin Pharmacol Toxicol.* 2022;130(5):606-617. doi:10.1111/bcpt.13722